New Insights into the Degradation Mechanism of Poly(vinyl chloride), Part II. Limited Polyene Sequence Length during Degradation and Synergism between Costabilizers

E. Santamaría,[1] M. Edge,[1] N. S. Allen,[1] H. B. Harvey,[2] M. Mellor,[2] J. Orchison[2]

[1]*Chemistry and Materials Department, The Manchester Metropolitan University, Chester Street, Manchester M1 5GD, United Kingdom*
[2]*Akcros Chemicals, Eccles Site, Research and Development, P.O. Box 1, Eccles, Manchester M30 OBH, United Kingdom*

Received 7 October 2003; accepted 23 February 2004
DOI 10.1002/app.20659
Published online in Wiley InterScience (www.interscience.wiley.com).

ABSTRACT: Fluorescence spectroscopy has shown that the limited sequence length exhibited during the thermal degradation of poly(vinyl chloride) (PVC) was the result of an HCl readdition/splitting off equilibrium, especially in unstabilized PVC formulations. In the case of stabilized PVC, the type and mechanistic action of the stabilisers seemed to play an important role in HCl re-addition. The possibility of a synergistic effect taking place between costabilisers for PVC, namely *N*-phenyl-3-acetyl pyrrolidine-2,4-dione (P24D) and its derivative *N*-isopropyl-*n*-phenyl-3-(1-iminoethyl) pyrrolidine-2,4-dione (P24D-d) has also been investigated by means of statistical design, degrading the samples at 170°C in air and measuring the induction time (T_i) of the degraded polymer. The results reveal that the stabilising efficiency is not only affected by the presence of the metal soap, but also by the nature of the substituents in the P24D derivatives. It may be concluded that P24D-d on degradation operates as a "reservoir" for P24D, extending the T_i to higher values compared to their individual performances and giving rise to a synergistic combination. The ability of the costabiliser to form a keto-enol tautomerism as well as its ability to interact with the PVC and the metal soap play a crucial role in controlling their stabilising effectiveness in the polymer. © 2004 Wiley Periodicals, Inc. J Appl Polym Sci 93: 2744–2763, 2004

Key words: poly(vinyl chloride); thermal degradation; stabilization; costabilizers; pyrrolidin-2,4-diones; fluorescence; design of experiments

INTRODUCTION

Poly(vinyl chloride) (PVC) has necessitated the use of organic costabilizers as adjuncts to the main stabilizer system. These compounds may be classified as long-term or short-term costabilisers. A short-term costabiliser provides good initial color to the system at the expense of reducing the induction time to degradation (e.g., the β-diketones: dibenzoyl methane, dehydroacetic acid), while a long-term costabiliser shows poor initial color but extends the induction time to degradation (e.g., pentaerythritol).

PVC degrades more rapidly when heated in air than when heated in an inert atmosphere. However, though the rate of dehydrochlorination (DHC) increases substantially, polymer discoloration is not as severe. Accelerated DHC is believed to be due to the abstraction of methylene hydrogen from the "intact" chain by peroxy radicals, thus initiating further DHC. This process induces both chain-scission and cross-linking via Diels- Alder cycloaddition. The fact that the presence of oxygen reduces the rate of color development suggests that oxygen either destroys the conjugated system or that oxygenated groups formed in the polymer block the unzipping reaction and hence reduce the extent of conjugation.

Hard experimental evidence is still lacking for the mechanism responsible for polyene formation, be it ionic[1–5] or radical[6–10] in nature. However, in the presence of oxygen, the presence of carbonyl groups is likely to influence the course of the degradation reaction. Panek et al.[11] have established the relatively low thermal stability of the *cis*-isomer of carbonylallyl chloride groups, using low molar mass model compounds. Svetly et al.[12–15] have studied the degradation of PVC in the presence of α,β-unsaturated ketones. The work proposed a mechanism in which the activating groups for the degradation are oxygen-contain-

Correspondence to: N. S. Allen (n.s.allen@mmu.ac.uk).
Present address for E. Santamaria: RIKA International Limited, C3 Brookside Business Park, Greengate, Middleton, Manchester M24 1GS, UK.

ing structures, which react with normal PVC units via a cyclic intermediate.

HCl abstraction from "intact" PVC is as probable as HCl abstraction adjacent to a polyene sequence, indicating that the "unzipping" reaction does not necessarily explain HCl elimination in PVC. Quantum mechanical calculations suggest a one-step elimination of approximately 22 HCl groups, a proposal consistent with polyene sequence length observed in practice.[16,17] The data suggest that, in solid-state, ionic reactions are preferred over radical ones. Semiempirical AM1 calculations suggest that the use of small unsaturated molecules as model compounds to simulate PVC degradation seems valid. The nature of the chain-ends influences the energetics and stability of polyene sequences.

From the literature it can be concluded that the polyene sequences are of limited length.[18] This is due to the following:

1. re-addition of HCl;
2. secondary reactions, such as Diels-Alder or intermolecular condensation;
3. and the fact that at certain polyene sequence lengths, elimination of HCl begins to become less thermodynamically feasible.

Van Hoang et al.[19,20] studied the readdition of HCl to predegraded PVC. It was shown that dehydrochlorination, although the predominant reaction during the early stages of degradation, is in competition with the readdition of HCl. The latter reaction becomes more significant as more double bonds are formed. Owen *et al.*[21] were also able to show evidence for the addition of HCl on predegraded PVC under ultraviolet irradiation, leading to a shortening of the polyene sequences. By using β-carotene as a model compound for conjugated dienes, Van Hoang et al.[22] proved by UV spectroscopy that the readdition of HCl to the polyene sequences led to the diminution of the long polyene sequences. Some authors also state that readdition shifts the average polyene length toward shorter polyenes.[23] Rasuvaev et al.[24] went even further and proposed a radical mechanism for the addition of HCl to conjugated double bonds. On the contrary, Guyot et al.[25,26] proposed an ionic mechanism. Nagy et al.[27] stated, however, that HCl can reinitiate the allyl-activated zip elimination by proton exchange with polyenes, leading to an increase in the average polyene length.

Fluorescence spectroscopy has been used in the study of various aspects of several polymers,[28–30] sometimes with a view to applying those results to the changes occurring in PVC and assessing the nature of the species forming. The use of luminescence spectroscopy as a tool to follow the formation of polyene sequences is well documented in the literature,[31] and proved to be much more successful, than, in particular, UV-visible spectroscopy, which showed not to be very sensitive due to the strong overlapping of bands of each polyene sequence, which make it difficult to calculate accurately the extinction coefficient for a given polyene length.[32]

There has been some speculation as to why the polyene sequences have limited lengths: since there is one branch for about 70 monomeric units and on average one linkage differing from the usual for about 50 monomeric units, these cannot cause the formation of short chains.[33] It has been suggested that, after a certain length of the polyene sequence is achieved, a state is reached at which an additional HCl split-off is no longer as energetically favorable as in the beginning. Some authors[34–36] have concluded that readdition of HCl occurred during degradation and that the limited polyene sequence length may have been the result of this equilibrium. Moreover, secondary reactions can stop the growth of the polyene sequences.

With a view to elucidating whether the readdition of HCl is responsible for the blocking of the sequence length, fluorescence studies of powder samples were carried out. For each formulation, samples that were degraded in air in a glass thimble will be commented upon first, then samples that were degraded in a closed degradation system. The latter, being in a closed system will allow the concentration of HCl to increase gradually. Both sets of results will be assessed and their results compared.

EXPERIMENTAL

Materials

PVC Solvic 271 GC, calcium stearate, zinc stearate, and P24D (*N*-phenyl-3-acetylpyrrolidin-2,4-dione) were supplied by Akcros Chemicals (Akzo Nobel).

Synthesis of *N*-isopropyl-*n*-phenyl-3-(1-iminoethyl) pyrrolidine-2,4-dione (P24D-d)

N-Phenyl-3-acetylpyrrolidine-2,4-dione (P24D) (10 g; 0.046 mol) was suspended in industrial methylated spirit (100 cm^3) until total solution. After the addition of isopropylamine (2.71 g; 0.046 mol), the reaction mixture was refluxed for 30 min. After refluxing, the solvent was removed by rotary evaporation. Diethyl ether was added to the mixture, which was then filtered and dried to yield a yellow solid (11.30 g, 95.2%), mp 165–168°C.

IR : ν (cm^{-1}) (KBr) : CN (1682)

δ_H (ppm) (CD_3OD) 1.4 (6H, d, $(CH_3)_2CH$), 2.5 (3H, s, CH_3C), 3.5 (1H, m, $CH(CH_3)_2$), 4.1 (2H, s, CH_2CO), 7.1

(1H, t, ArH(p)), 7.4 (2H, t, ArH(m)), 7.7 (2H, d, ArH(o)).

Degradation of samples

A glass tube containing 500 mg of each sample was degraded for 5, 10, 15, 20, 25, and 30 minutes at 170°C in an oil bath. After heating, the samples were left to cool down at room temperature for posterior analysis.

For the HCl readdition, a closed system was used, without the removal of HCl, thus allowing the HCl concentration to increase gradually.

Fluorescence analysis

Samples were analyzed using a Perkin Elmer LS 55 Luminiscence Spectrometer, (accurately weighed mass: 0.05g) with an excitation/emission slit width of 7.5 nm and a scan speed of 800 nm/min.

Design of experiments (DOE)

The package used was a Stat-Ease Design-Expert®Software, Version 5.0

The term experimental design is usually used to describe the stages of identifying the factors, which may affect the results of a experiment, designing the experiment, so that the effects of uncontrolled factors are minimized and using statistical analysis to separate the effects of various factors involved.

Two different types of designs were carried out:

1. Response surface methodology (RSM) is a collection of mathematical and statistical techniques with the objective of optimizing the response. The first step in RSM is to find an approximation of the true relationship between the response and the set of independent variables. The response is usually modeled by a low-level polynomial (first order or second order) that usually works relatively well under a relatively small region. Contour plots play a very important role in response surface methods. By use of this technique, one can characterize the shape of the surface and locate the optimum with reasonable precision
2. Full factorial design, which allows the estimation the main effects and two-factor interaction separately. Factorial designs allow the effects of a factor to be estimated at several levels of the other factors, yielding conclusions that are valid over a range of experimental conditions.

Induction time (T_i) to dehydrochlorination measurements

A glass tube containing 500 mg of the sample was introduced in an oil bath at 170°C. A stream of preheated air (60 ml/min) was introduced by an air pump, which swept the evolved HCl into a cell containing 100 ml of 0.1*M* KCl solution. The electrical potential of this solution was continuously monitored with time. The induction time was calculated as the period prior to a rapid change in potential and was obtained graphically by the intersection of the two best lines fit to the curves. Initial degradation rates were also obtained as the slope of the best line to fit the curve. After heating, the samples were left to cool down at room temperature.

RESULTS AND DISCUSSION

Fluorescence studies

For control PVC at the excitation wavelength of 270 nm (Fig. 1), the emission spectrum before degradation showed a band at 310 nm that has been attributed either to build-up of short polyenes sequences[37] or to carbonyl groups present in the starting material, residues of catalysts. According to Rabek et al.,[38] this emission band is ascribed to different carbonyl group impurities that are impossible to remove, indicating that they are permanently attached to the PVC. This argument is in line with the observations of Allen,[39] who proposed that the α,β-unsaturated carbonyl groups were responsible for the initial fluorescence. Similar results to those shown here were obtained by Owen and Read,[40] who pointed out that a diene contained in a rigid skeleton could be the structure involved.

On degradation this band decreased its intensity due to the disappearance of these short polyene sequences, which evolved to form longer sequences. This increase in the polyene sequence distribution was also accompanied by a pinkish coloration of the samples. In addition, sequences arising in the early stages of degradation, such as the emission band at 360 nm (5 min) and especially the band centerd at 380 nm (10 min), appeared to grow stronger as the degradation proceeded. After 30 min, short polyene sequences were no longer present and, judging by the broadness of the band at 380 nm, the length of the newly conjugated sequences formed was subject to mixtures.

At a higher excitation wavelength (Fig. 2), there was no emission band prior to degradation, which supported the fact that there were no long polyene sequences in the control sample. On degradation, there was strong evidence of the formation of sequences of different lengths and/or different species (shoulders at around 380, 410, and 440 nm), which led to the formation of a broad band that decreased its intensity quite substantially after 30 min. This could suggest that, after the long polyene sequences reach a certain length, they undergo secondary reactions such as cyclization and in some cases Diels-Alder reaction that

Materials

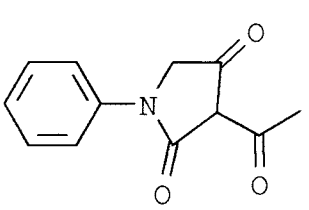

P24D

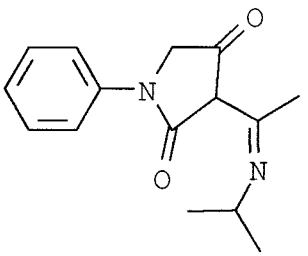

P24D-d

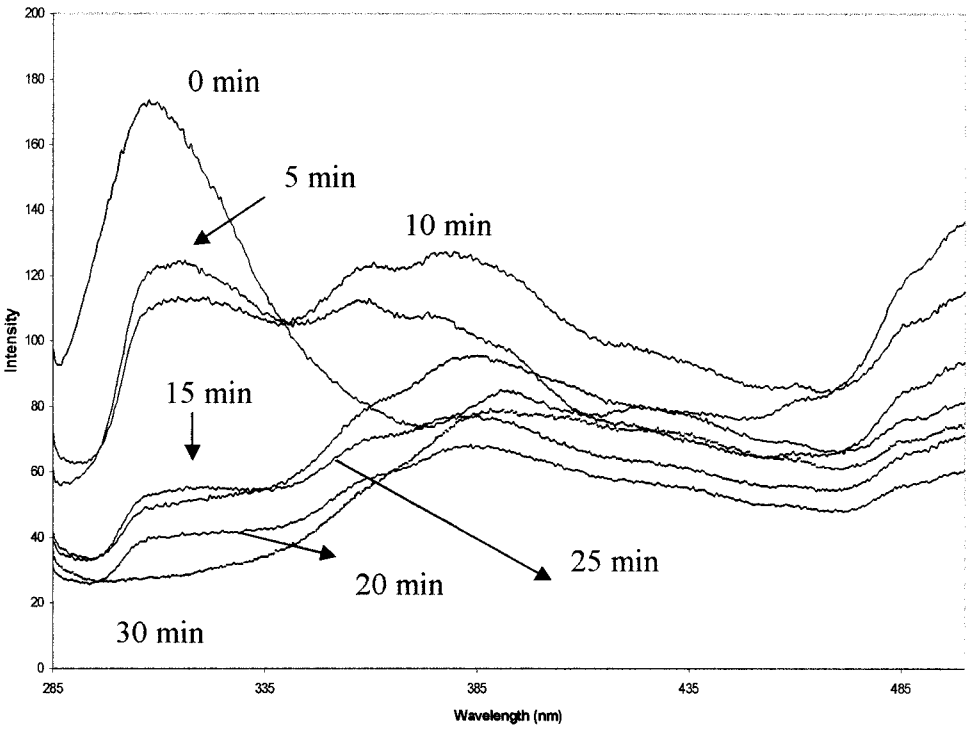

Figure 1 Control PVC for excitation wavelength $\lambda = 270$ nm.

can disrupt the growing polyene sequences and cause the decrease in the intensity of the emission bands.

By way of contrast, the following spectra in Figures 3 and 4 show changes in the sequence length of samples that were degraded in a closed system with a view to elucidating whether the readdition of HCl actually takes place.

Prior to degradation, the emission spectrum in Figure 3 showed a strong emission band centerd at 310 nm assigned to short polyene sequences or α,β-unsaturated carbonyl groups. On degradation, the intensity of this band decreased sharply compared to its counterpart in Figure 1, which suggested that the initial short sequences grew very rapidly, catalyzed by the presence of HCl. It was also observed in Figure 1 that, in later stages of degradation, longer sequences were formed, but in this instance the broadness of the band since early stages on the one hand, and the lack of shoulders at lower wavelengths on the other, seemed to imply that the sequence length grew very rapidly as a result of the catalytic role of HCl. Similar results were obtained by Patel et al.[41] who came to the conclusion that autocatalysis was an integral feature of the solid-state thermal degradation of PVC.

At the excitation wavelength of 340 nm (Fig. 4), before degradation there were no significant emission bands. On degradation, an emission band centerd at 440 nm arose together with another band of lower intensity based at 410 nm. However, it was only after 10 min that the emission band based at 440 nm

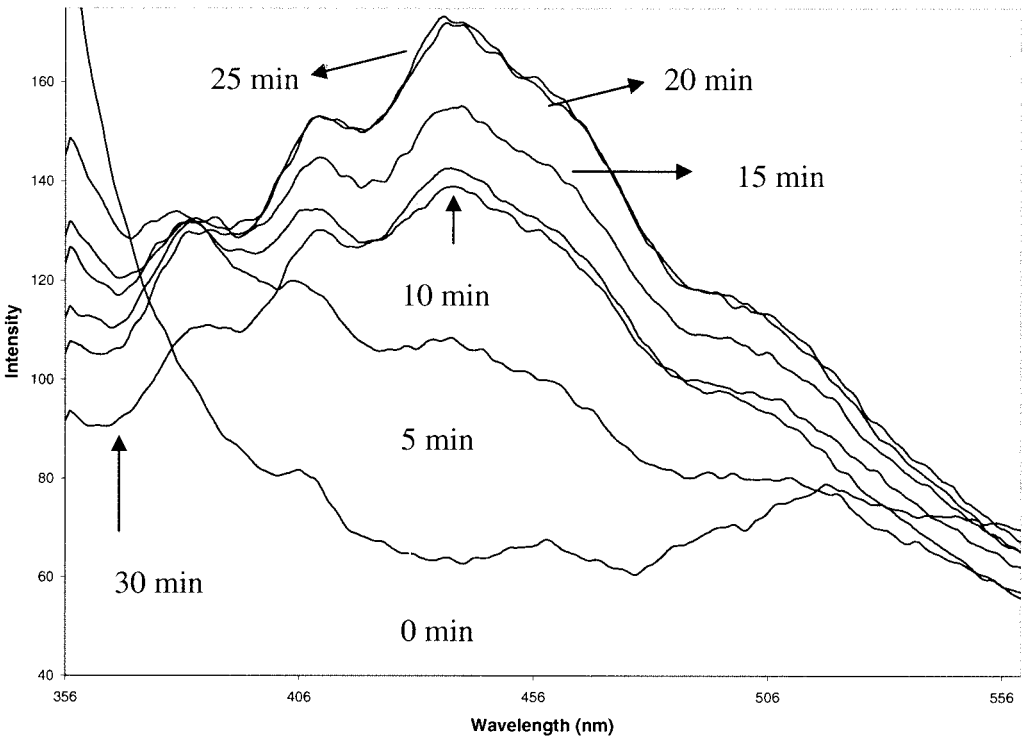

Figure 2 Control PVC for excitation wavelength $\lambda = 340$ nm.

reached its maximum compared to 25 min in the open system (Fig. 2). Furthermore, after 15 min the intensity of the band started to increase again up to 25 min, where it seemed to, again, reach this maximum length.

Since the main aim of this section was to shed light on the cause of the limited length of the polyene sequences, our results suggest that in unstabilised PVC there is readdition of HCl taking place and that the limited sequence length is the result of this HCl readdition/splitting-off equilibrium. On the whole, the catalytic effect of HCl can be seen to be improved from the long polyene sequences formed in samples

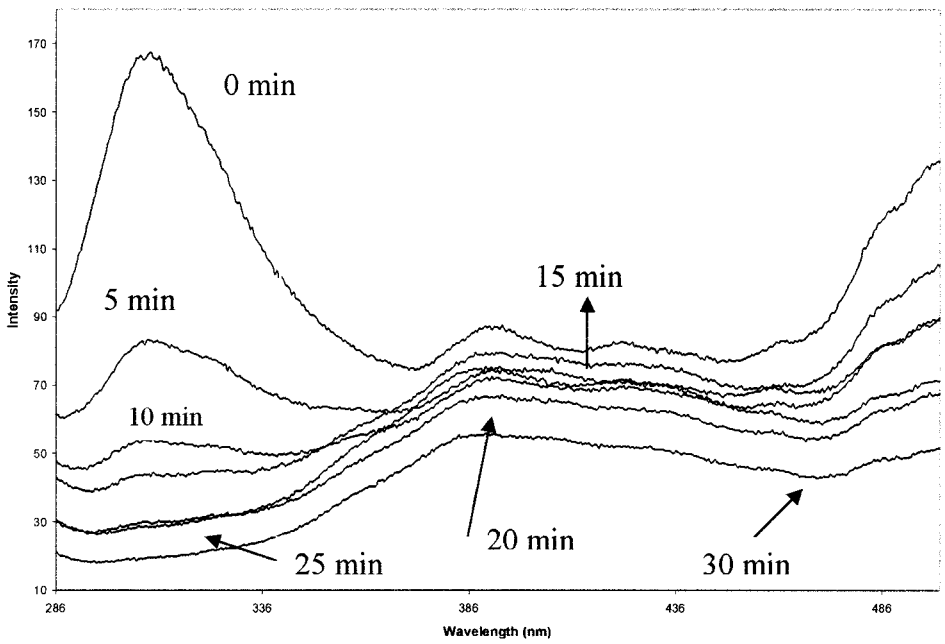

Figure 3 Readdition of HCl in control PVC for excitation wavelength $\lambda = 270$ nm.

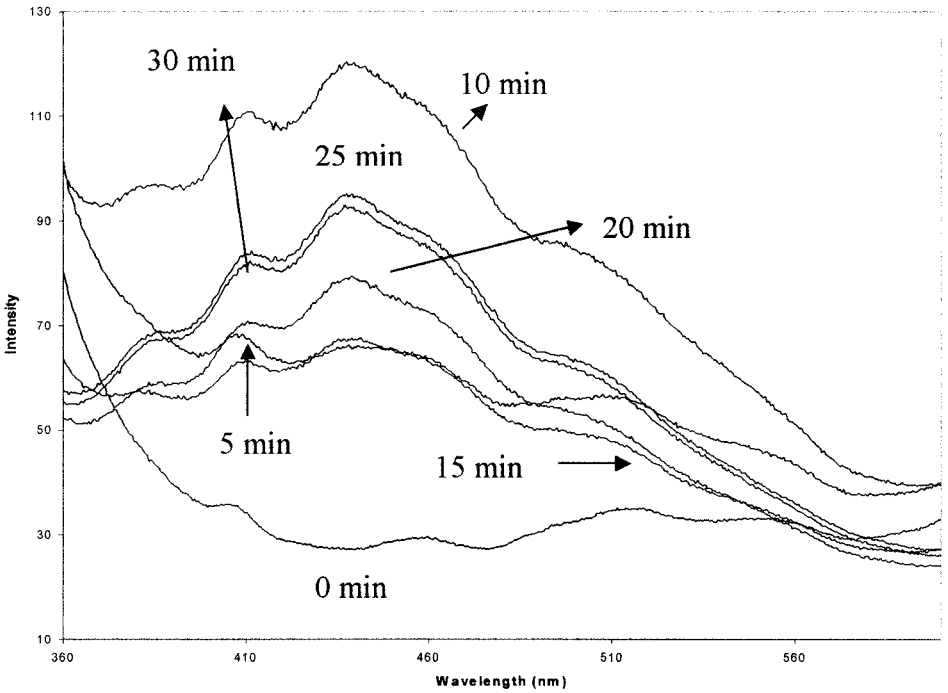

Figure 4 Readdition of HCl in control PVC for excitation wavelength $\lambda = 340$ nm.

degraded in the closed degradation system (Fig. 4). After 10 min of degradation, the polyene sequence seemed to have reached a certain length (more quickly than the control sample in Fig. 2 due to the catalytic effect of HCl), where an additional HCl split-off was not favorable, and it is probably then when the readdition of HCl takes place (sharp decrease in intensity of band at 440 nm). Van Hoang *et al.*[42,43] have already suggested that the readdition of HCl becomes more important as double bonds are formed. It's unlikely that secondary reactions occur at this early stage in the degradation process. The re-addition of HCl results in the shortening of the polyene sequence distribution, and this effect manifests itself in the reduction in the intensity of the longer sequences. Later on, the sequence length starts growing up again until the energy required for HCl splitting-off is equal to the delocalization energy of the polyene sequence, so the readdition of HCl takes place and the same effect happens all over again. Accordingly, for shorter polyene sequences (310 nm λ_{ex} 270 nm), the dramatic decrease in the intensity of the emission spectra is related to the catalytic effect of the evolved HCl, which promotes the extension of the polyene chain, thus reducing its concentration within the polymer chain.

For a PVC stabilized formulation containing P24D, 0.3 phr at the excitation wavelength of 270 nm (Fig. 5), prior to degradation the broad emission band centerd at 420 nm can be attributed to the presence of P24D. On degradation a slight shift toward higher wavelengths (435 nm) can be observed due to its interaction with the PVC chain. Although Zn^{2+} is required to confer P24D the planarity necessary for the C-alkylation reaction (See Part 1), part of P24D can still interact with the PVC chain. The intensity of the emission band decreases on degradation, suggesting that the complex P24D–PVC chain breaks up during the degradation process.

At a higher excitation wavelength (Fig. 6), the emission band prior to degradation corresponded to P24D. Again, on degradation there is a shift toward higher wavelengths (440 nm) due to the interaction of P24D–PVC. The sudden drop in the intensity after 10 min is attributed to the decomposition of the complex. The broad nature of the band suggests the formation of polyene sequences of different lengths.

Similar results to those shown in Figure 5 were obtained in the case of the closed degradation system for an excitation wavelength 270 nm. At the excitation wavelength of 340 nm (Fig. 7), the emission bands obtained were also very similar to those in Figure 6. The only difference was that, due to the readdition of HCl onto the polyene sequences, the intensity of the emission band started to decrease earlier than in the control sample (Fig. 6), which indicated the shortening of the polyene sequences taking place.

In an earlier work,[44,45] it was reported that the following reaction could take place:

The decomposition products of P24D-d, are an amine gas and a compound with a structure very similar to P24D.

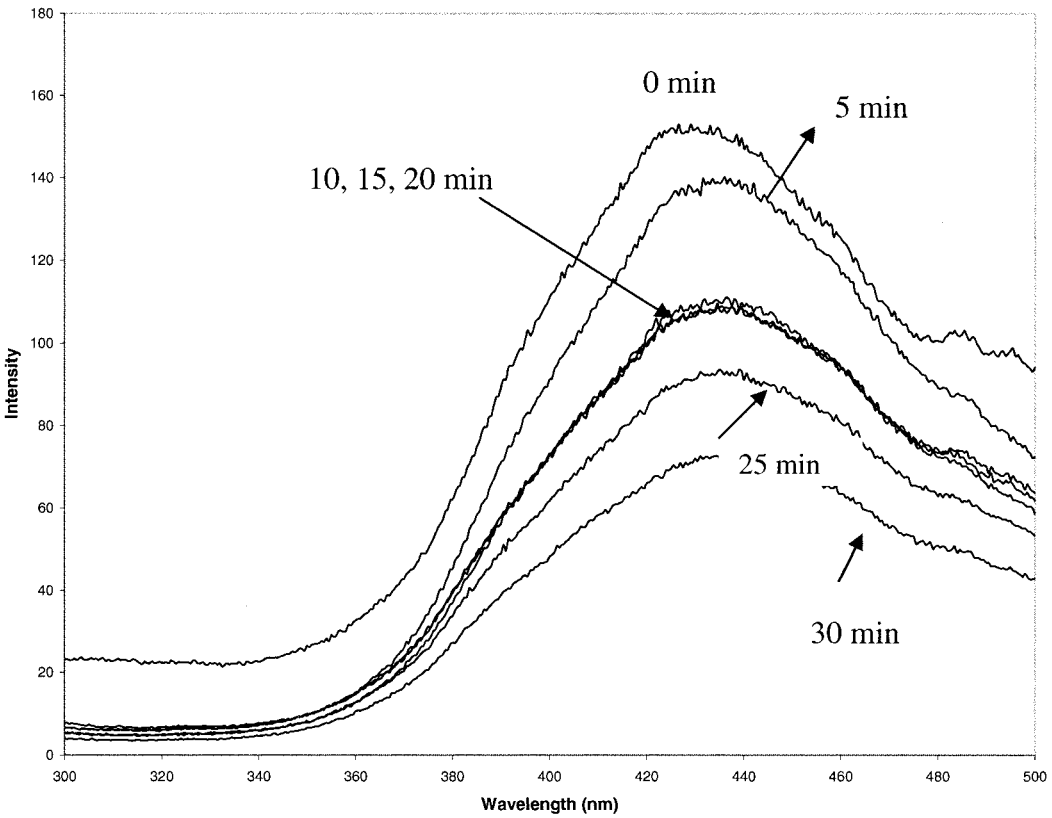

Figure 5 PVC + P24D 0.3 phr for excitation wavelength λ = 270 nm.

In the case of a PVC stabilised formulation containing P24D-d 0.3 phr, at the excitation wavelength of 270 nm, Figure 9 shows a broad and strong emission band at 420 nm before degradation due to the presence of P24D-d. The shoulder at 310 nm is again attributed to short polyene sequences or α,β-unsaturated carbonyl

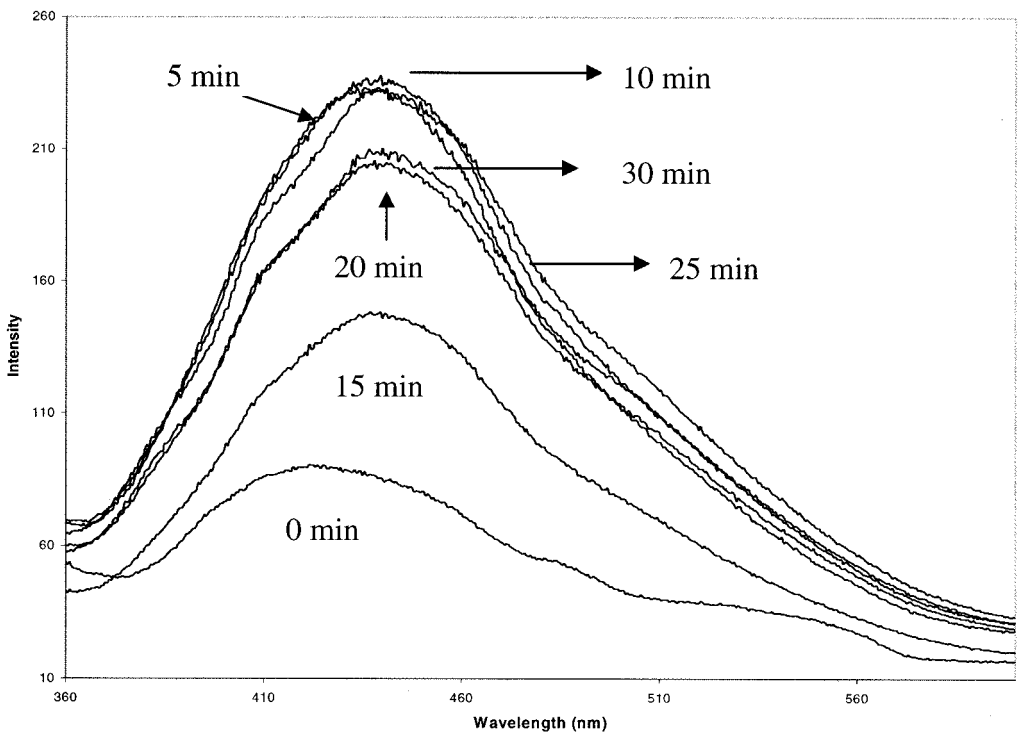

Figure 6 PVC + P24D 0.3 phr for excitation wavelength λ = 340 nm.

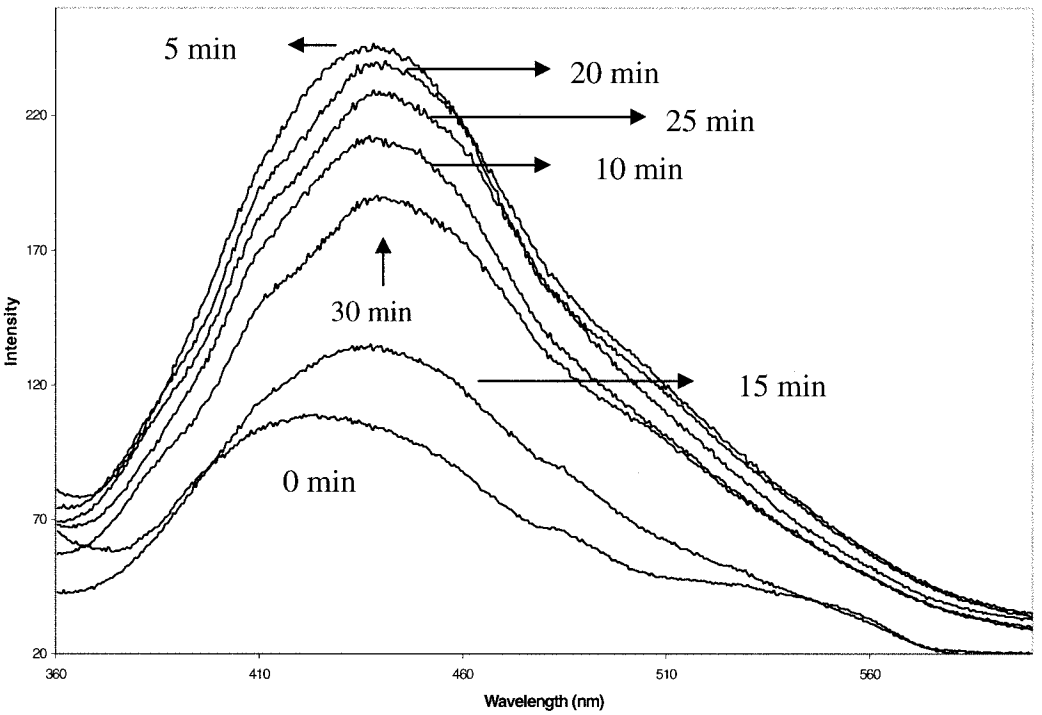

Figure 7 Readdition of HCl in PVC + P24D 0.3 phr for excitation wavelength λ = 340 nm.

groups. On degradation, this band shifts slightly toward higher wavelengths (430 nm) in what appears to be the locking of the co-stabiliser across the short polyenes to form a fluorescent complex. The shoulder at 310 nm seems to disappear in the very early stages of degradation, while the intensity of the main band decreases on further degradation.

At the excitation wavelength of 340 nm, the emission spectrum before degradation (Fig. 10) shows a broad band centerd at 410 nm that can be assigned to P24D-d. On degradation, this band shifts toward 440 nm, implying that P24D-d forms a fluorescent complex with PVC. As well as shifting, this band also increases its intensity, which leads to the suggestion that increasing amounts of long polyene sequences are being formed.

With regard to the samples degraded in the closed system, no changes were observed at an excitation wavelength of 270 nm. As for the excitation wavelength of 340 nm (Fig. 11), the growth of the polyene sequences seemed to stop earlier than in the control (Fig. 10), suggesting that the readdition of HCl occurs, resulting in the formation of shorter sequences.

If these results are compared to those obtained with P24D, it can be clearly observed that the evolution of higher concentrations of long polyene sequences (λ_{ex} = 340 nm) in the case of P24D-d can be attributed to the amine gas released on decomposition of P24D-d, which neutralizes the HCl evolved, thus delaying the readdition of HCl onto the polyene sequences.

For the formulation containing PVC + preheated mixture Ca/Zn stearates (2 : 1) 3 phr, at the excitation wavelength of 270 nm (Fig. 12), the emission spectrum prior to degradation shows a band at 310 nm assigned to short polyene sequences or α,β-unsaturated carbonyl groups and a band of higher intensity at about 390 nm. This latter band is attributed to the complex

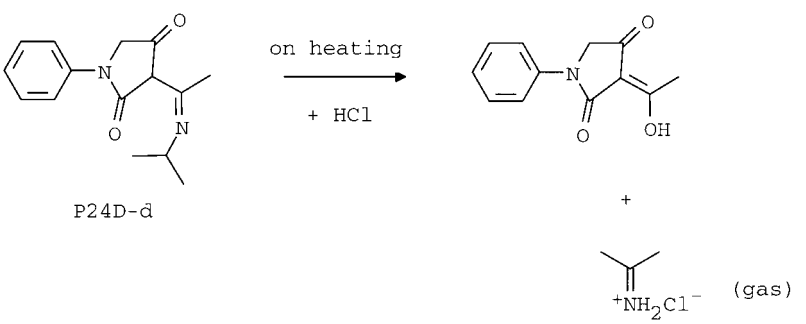

Figure 8 Decomposition of P24D-d on heating.

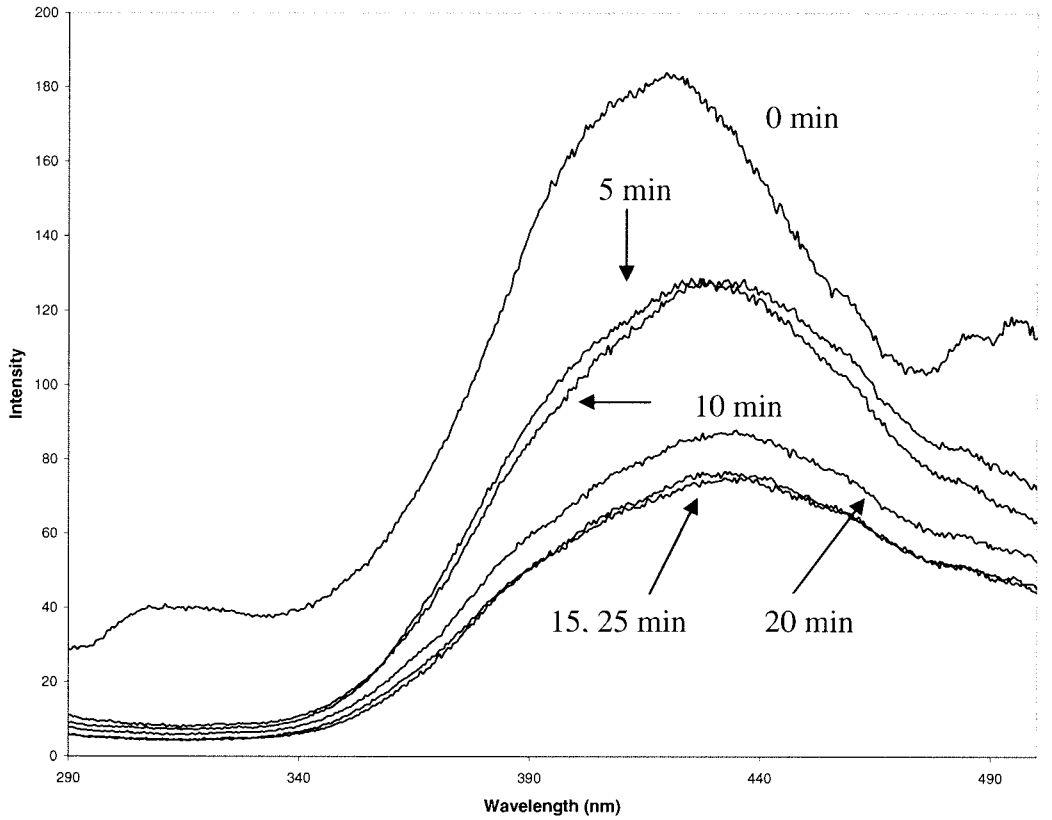

Figure 9 PVC + P24D-d 0.3 phr for excitation wavelength λ = 270 nm.

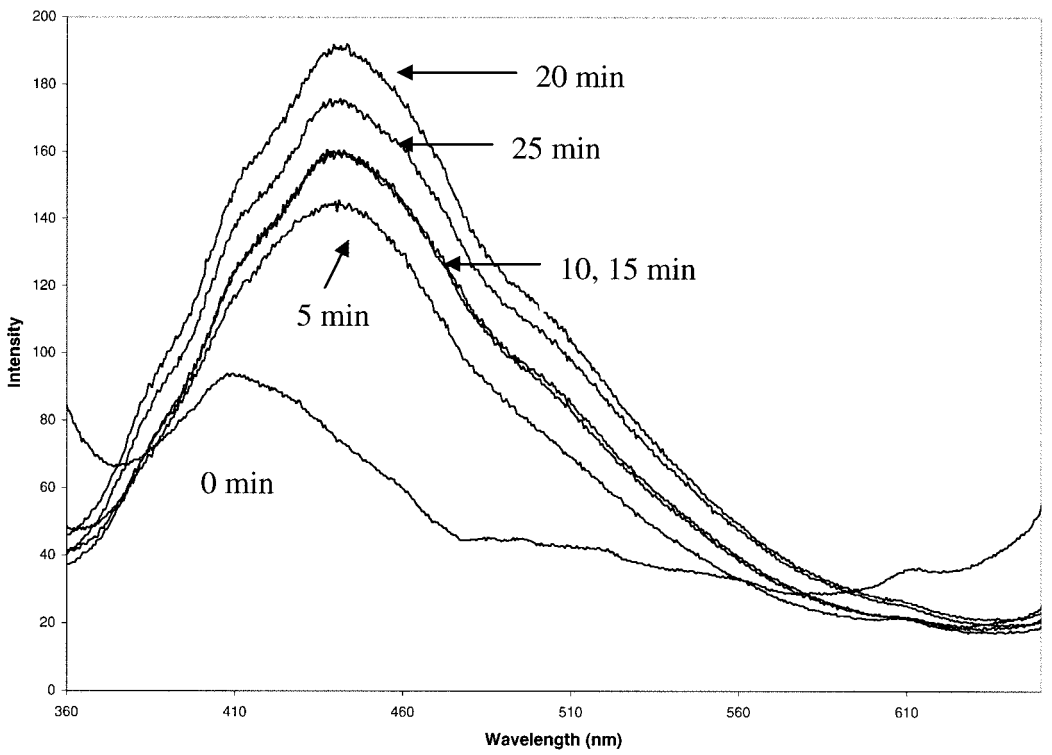

Figure 10 PVC + P24D-d 0.3 phr for excitation wavelength λ = 340 nm.

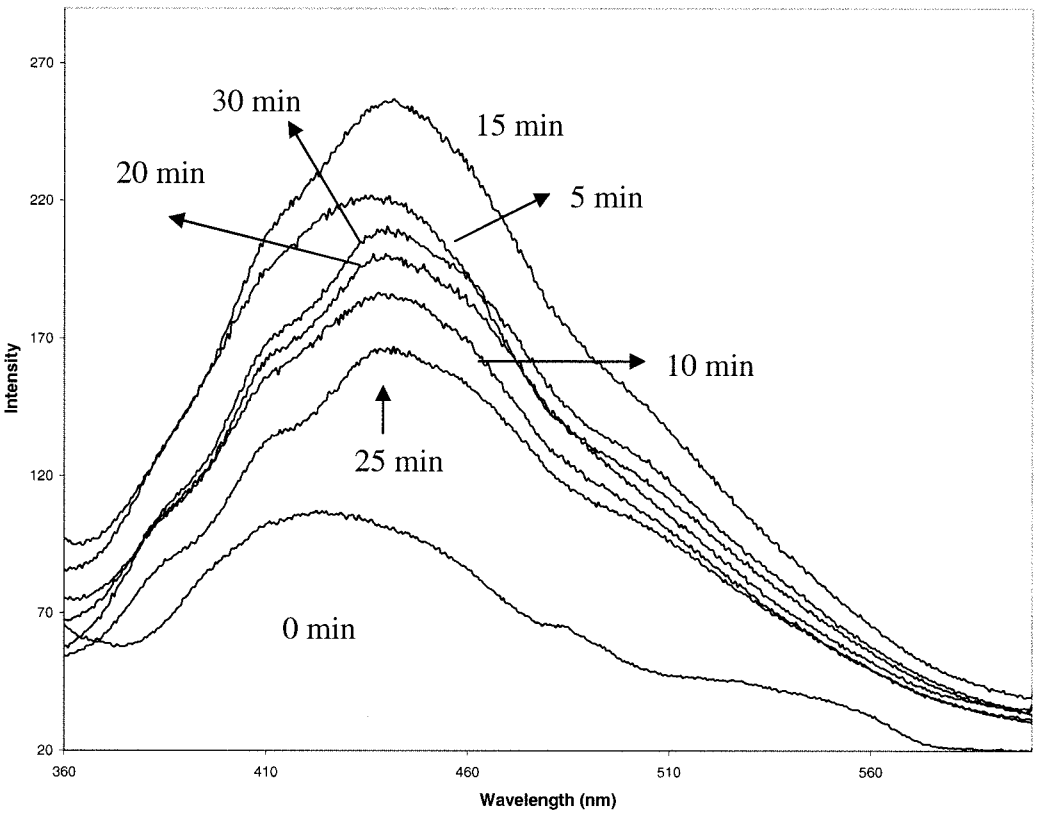

Figure 11 Readdition of HCl in PVC + P24D-d 0.3 phr for excitation wavelength λ = 340 nm.

$CaSt[ZnSt_3]$[46] of the preheated mixture of Ca/Zn stearates. On degradation, the band at 310 nm weakens as longer sequences are formed. At the same time, the band at 390 nm shifts slightly toward shorter wavelengths (380 nm). This can be attributed to the interaction complex $CaSt[ZnSt_3]$–PVC.

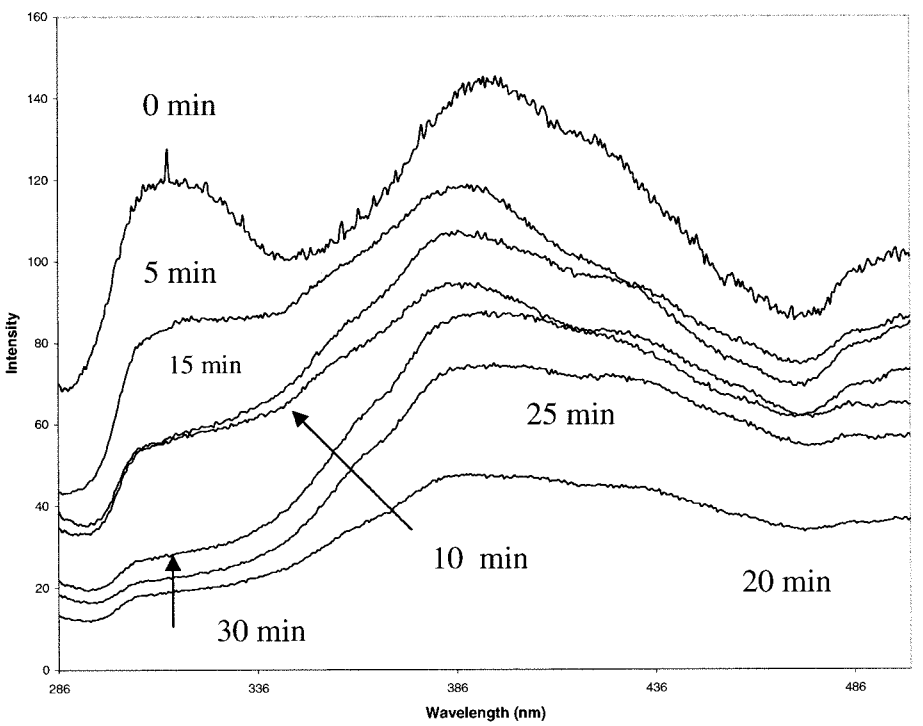

Figure 12 PVC + preheated mixture Ca/Zn 3 phr for excitation wavelength λ = 270 nm.

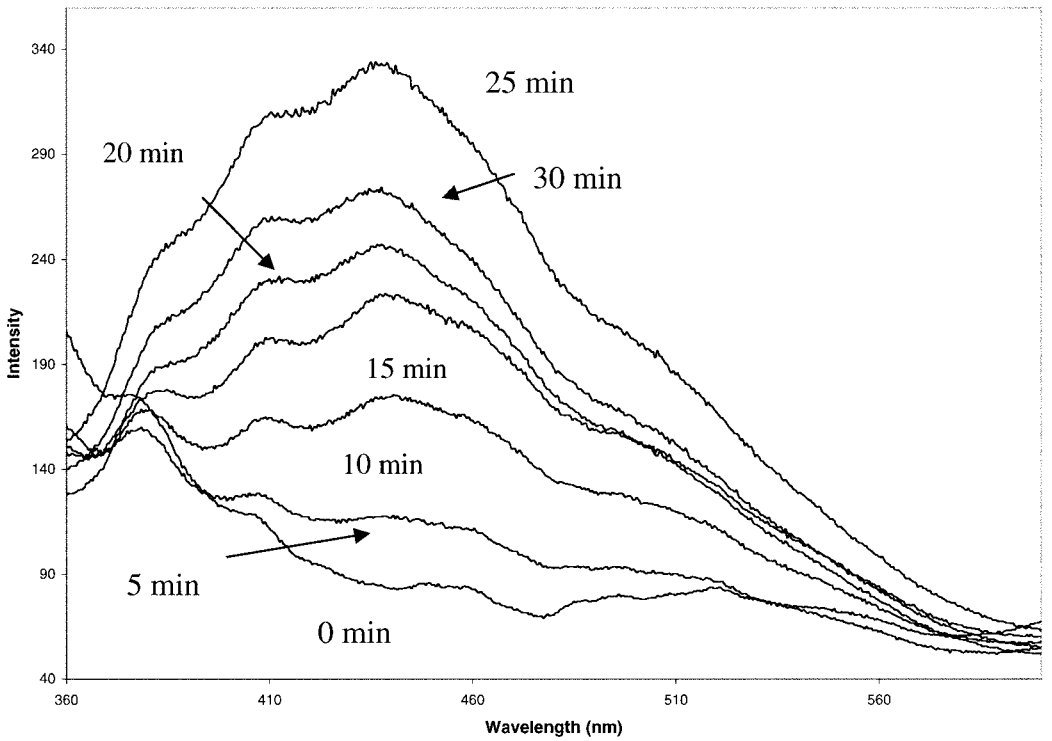

Figure 13 PVC + preheated mixture Ca/Zn 3 phr for excitation wavelength $\lambda = 340$ nm.

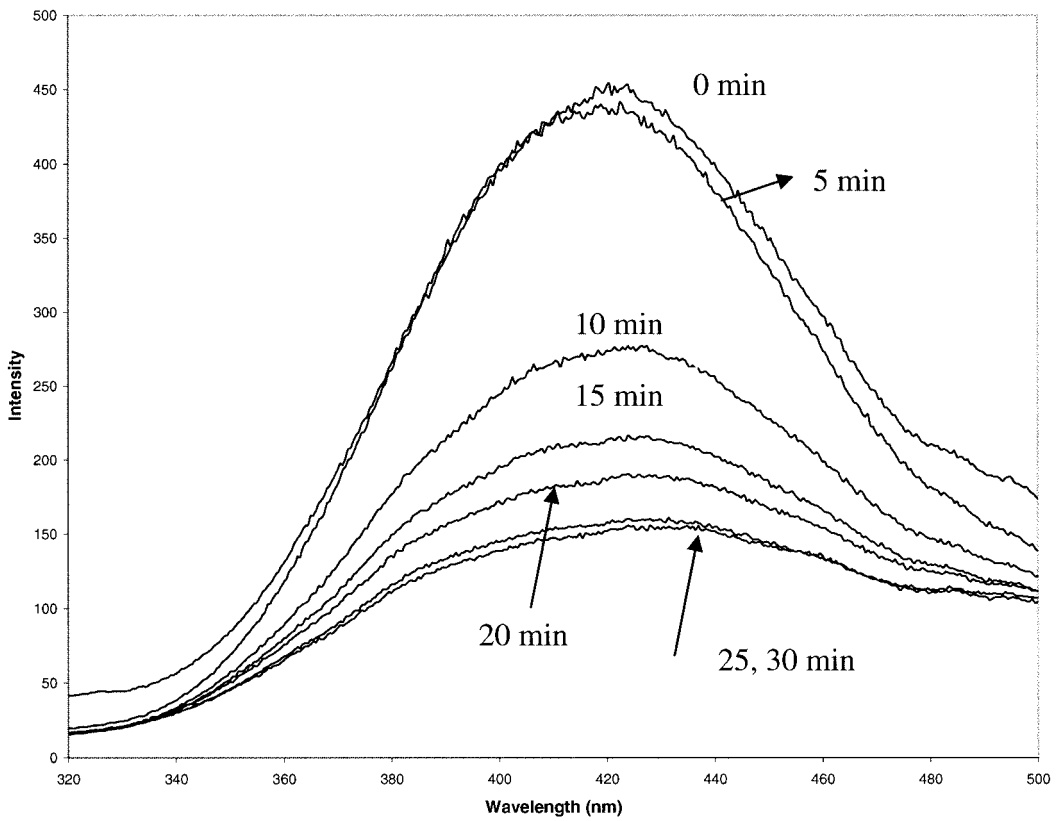

Figure 14 PVC + preheated mixture Ca/Zn 3 phr + P24D 0.3 phr for excitation wavelength $\lambda = 270$ nm.

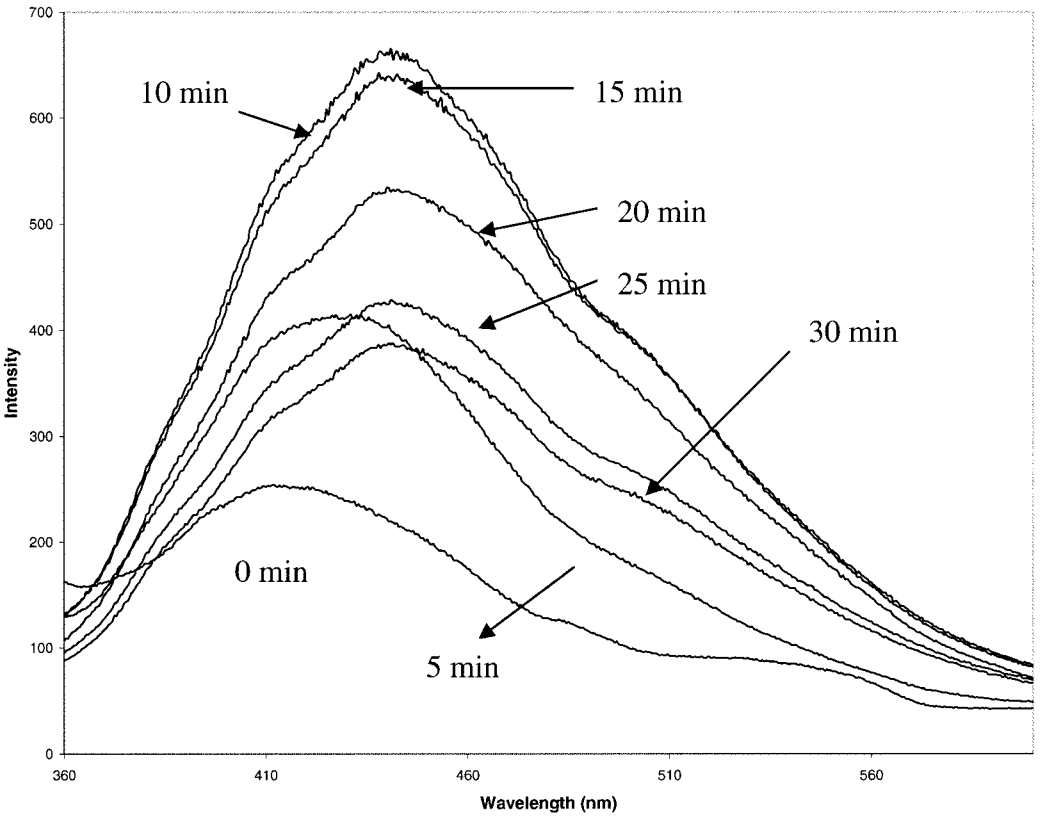

Figure 15 PVC + preheated mixture Ca/Zn 3 phr + P24D 0.3 phr for excitation wavelength $\lambda = 340$ nm.

After 15 min, there is a dramatic drop in the intensity, probably due to the breaking up of the complex.

In Figure 13 the emission bands at the excitation wavelength of 340 nm are depicted. The most striking feature is the development, upon degrada-

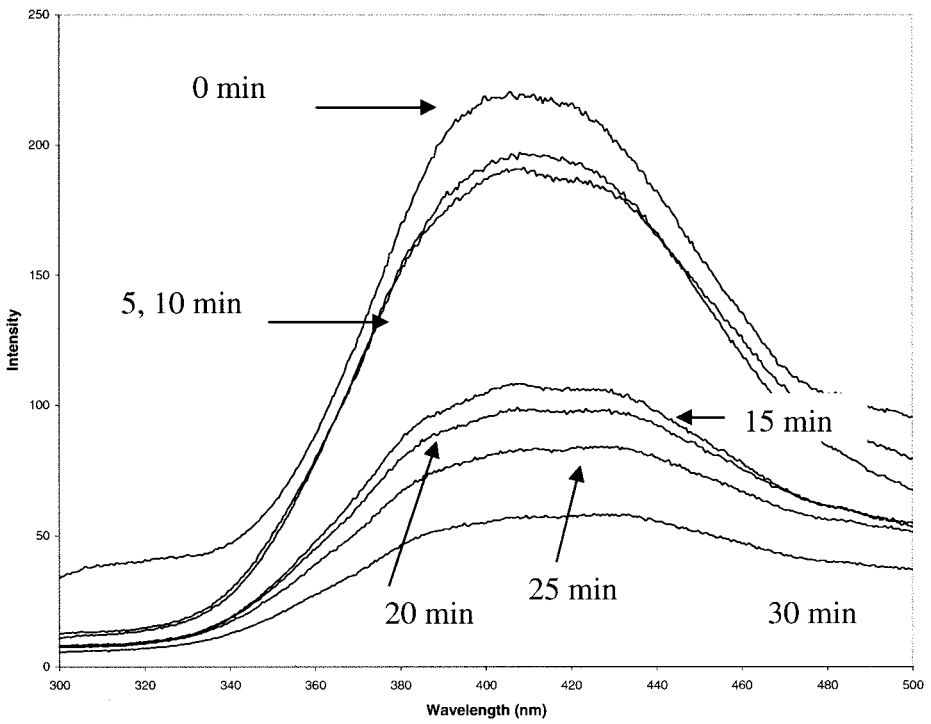

Figure 16 PVC + preheated mixture Ca/Zn 3 phr + P24D-d 0.3 phr for excitation wavelength $\lambda = 270$ nm.

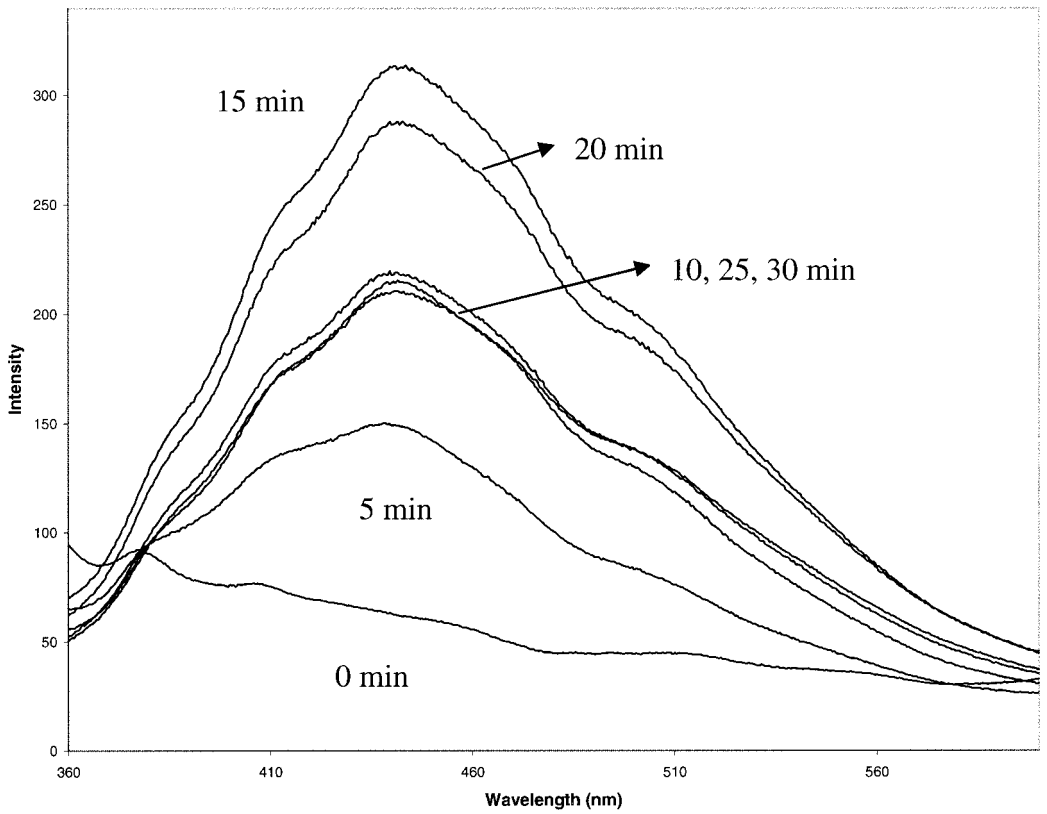

Figure 17 PVC + preheated mixture Ca/Zn 3 phr + P24D-d 0.3 phr for excitation wavelength λ = 340 nm.

tion, of three bands based at 380, 410, and 440 nm. It's worth noting at this stage that the bands at 380 and 410 nm seemed less defined as opposed to those in Figure 2 for the PVC control. This can be attributed to the substitution of labile structures in the PVC chain by zinc stearate, resulting in

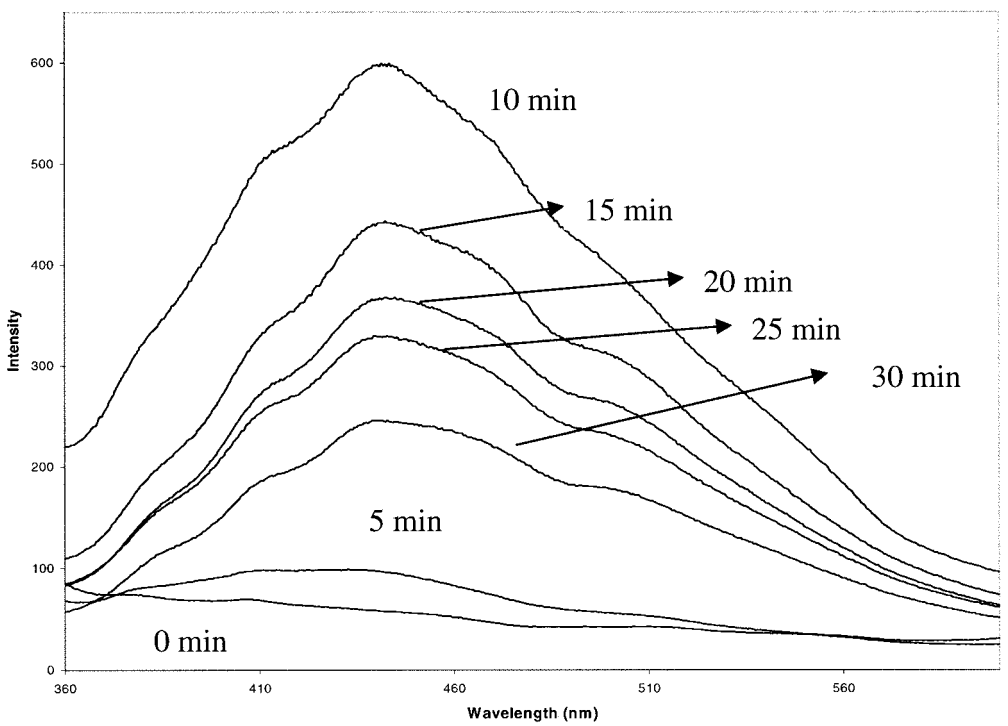

Figure 18 Re addition of HCl in PVC + preheated mixture Ca/Zn + P24D-d 0.3 phr for excitation wavelength λ = 340 nm.

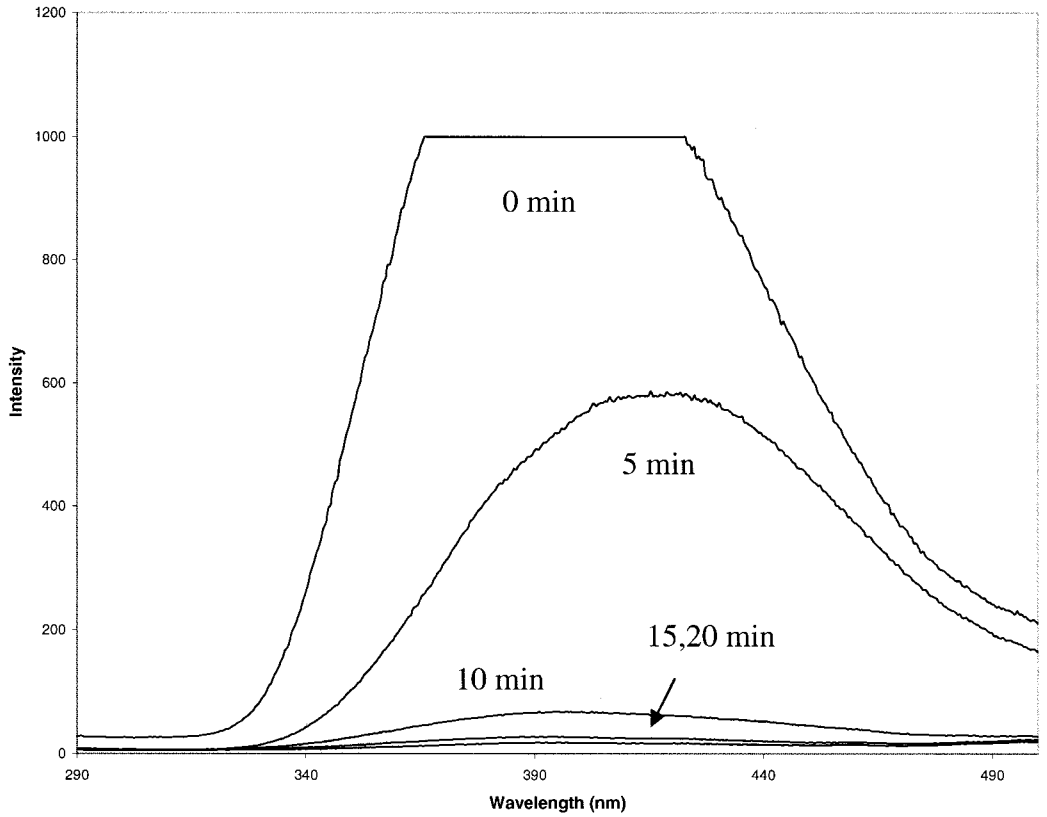

Figure 19. PVC + $ZnSt_2$ 3 phr + P24D 0.3 phr for excitation wavelength $\lambda = 270$ nm.

a lower concentration of long polyene sequences formed. Moreover, the decrease in the intensity of the band after 25 min bore strong resemblance to PVC control (Fig. 2), where it was suggested that *intra-* and *inter*molecular cyclizations started taking place.

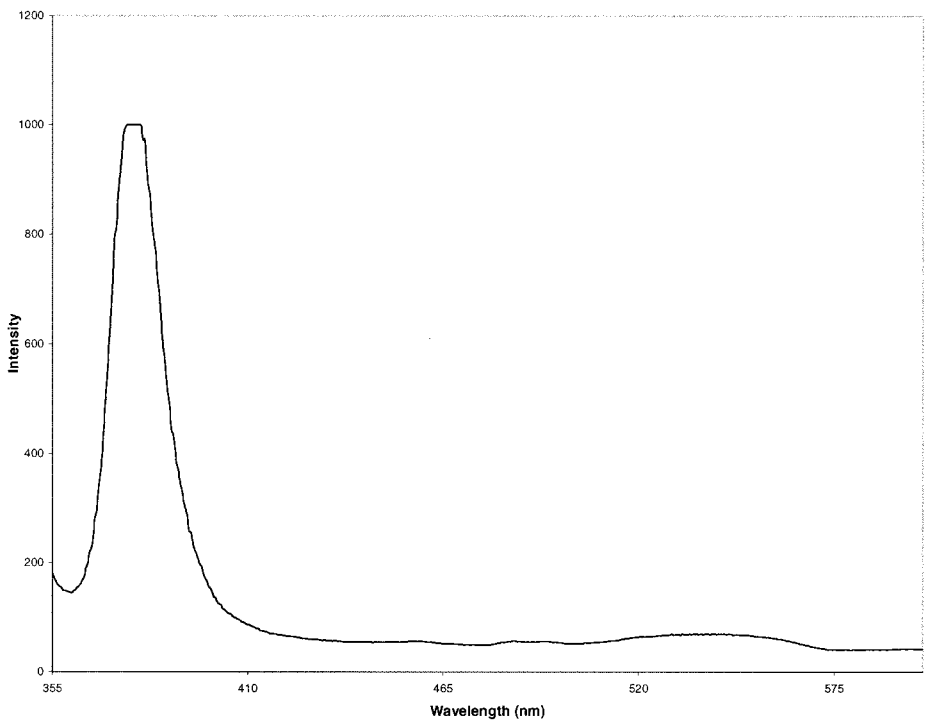

Figure 20 $ZnSt_2$ alone for excitation wavelength $\lambda = 340$.

TABLE I
Design Summary for RSM P24D–P24D-d

Study type		Response Surface		Experiments 18
Initial design		Central Composite		Blocks 2
Design model		Quadratic		
Response name		Units		
Induction time		min		
Factor	Name	Units	Low Actual	High Actual
A	P24D	phr	0.000	1.00
B	P24D-d	phr	0.000	1.00

In the case of the closed degradation system, similar results to those shown in Figures 12 and 13 were obtained. This indicates that, during the period of analysis, with Ca and Zn stearates being HCl scavengers, there was not enough HCl evolved to reattach the polymer sequences.

When 0.3 phr of P24D was added to the previous formulation, before degradation (Fig. 14) there is a very strong and broad band at 420 nm due to both the complex CaSt[$ZnSt_3$] and P24D. On degradation, the band dramatically decreased its intensity due to consumption of the stabilizers, with no obvious shift in the wavelength.

In Figure 15, the emission band prior to degradation at 420 nm is due to P24D, as the metal soaps do not fluoresce (Fig. 13). On degradation, there is a shift toward higher wavelengths (440 nm), attributable to the complexation between P24D and zinc stearate that in later stages participates in the C-alkylation reaction. After 10 min the intensity of the band decreases in what seems to be a sign of the shortening of the polyene sequence distribution following the blocking of the long polyene sequences by P24D.

A comparison between these emission spectra and those exhibited in Figure 13 demonstrates again that P24D acts as a short-term costabilizer blocking or interrupting the propagation of the polyene sequence that leads to the improvement of the initial colouration.

The emission spectra obtained for the closed degradation system at both excitation wavelengths were very similar to those shown below and have not been included.

When 0.3 phr of P24D-d was added to the formulation, Figure 16 showed a strong band at 410 nm, before degradation, due to both the complex of metals soaps and P24D-d. On degradation, the intensity of the band decreased due to the consumption of stabilisers.

At a higher excitation wavelength (Fig. 17), prior to degradation there are no significant emission bands. In later stages of degradation, there is the evolution of a band centerd at 440 nm, which may indicate the decomposition of P24D-d and the formation of a complex via C-alkylation in the presence of metal soaps. After 15 min the intensity of the band starts to decrease, suggesting the formation of shorter polyenes following the locking of P24D-d across the PVC chain.

When the same samples were degraded in the closed degradation system, similar results were obtained for the lower excitation wavelength.

At the excitation wavelength of 340 nm (Fig. 18), the intensity of the band started to decrease earlier compared to Figure 17; a fact that points to the formation of shorter polyene sequences following the readdition of HCl.

The figures show the excitation spectra obtained when 3 phr of zinc stearate and 0.3 phr of P24D were added to PVC.

At the excitation wavelength of 270 nm (Fig. 19), prior to degradation the saturated emission band at around 390 nm is attributed to the planarity of the complex Zn^{2+}–P24D (see Part 1). It seems that this complexation takes place even on simple mixing. After 5 min the band shifts toward higher wavelengths, which can be attributed to the C-alkylation reaction between P24D and PVC. The sudden decrease in the intensity of the band is accompanied by a rapid blackening of the sample due to the evolution of $ZnCl_2$.

Before degradation at the excitation wavelength of 340 nm (Figure 19), there is a sharp peak at 380 nm

TABLE II
Model Statistics Summary for RSM P24D–P24D-d

Source	Root MSE	*R*-squared	Adjusted *R*-squared	Predicted *R*-squared	PRESS
Linear	6.31	0.6631	0.6150	0.4252	949.93
Quadratic	4.23	0.8808	0.8266	0.7129	474.48

TABLE III
Equation for Quadratic Model for RSM P24D–P24D-d

T_i (induction time) =	+16.55
	+23.28 × P24D
	−13.12 × P24D-d
	$-20.30 \times P24D^2$
	$+24.31 \times P24D\text{-}d^2$
	+7.00 × P24D × P24D-d

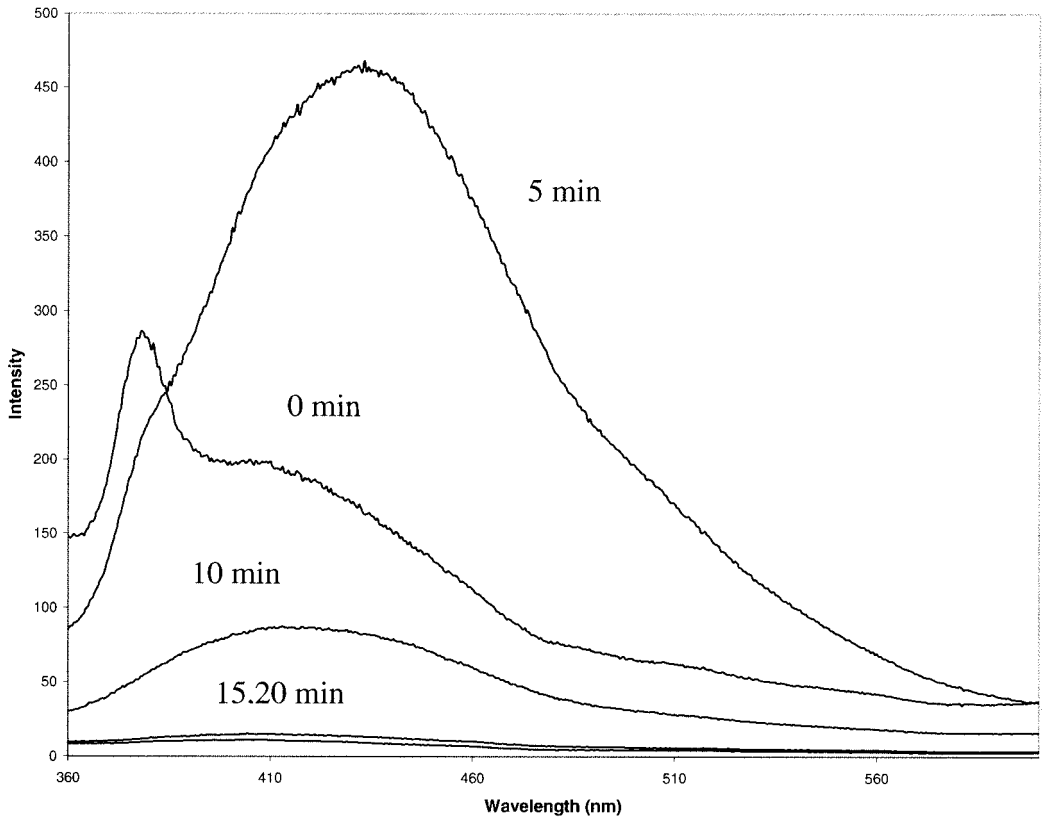

Figure 21 PVC + $ZnSt_2$ 3 phr+ P24D 0.3 phr for excitation wavelength $\lambda = 340$ nm.

that is assigned to the presence of impurities in the zinc stearate (Figure 20). On degradation the band becomes more intense and broad and is centerd at 440 nm, due to the P24D–PVC complex. After 10 min, the intensity of the band decreases dramatically and shifts toward lower wavelengths, which may be due to the decomposition of the complex (Figure 21). Moreover, the catalytic effect of the $ZnCl_2$ evolved leads to the catastrophic blackening of the polymer and, thus, the dramatic decrease in the intensity.

The samples degraded in the closed degradation system showed the same emission bands. In fact, the

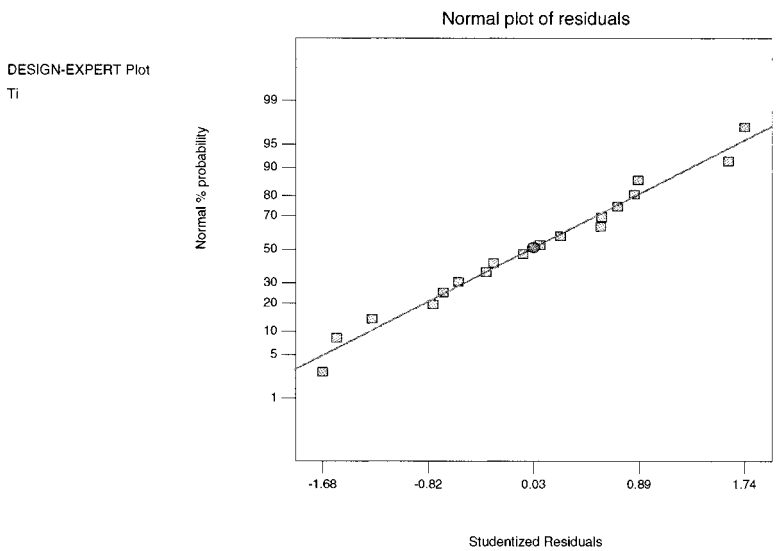

Figure 22 Plot of residuals for RSM P24D–P24D-d.

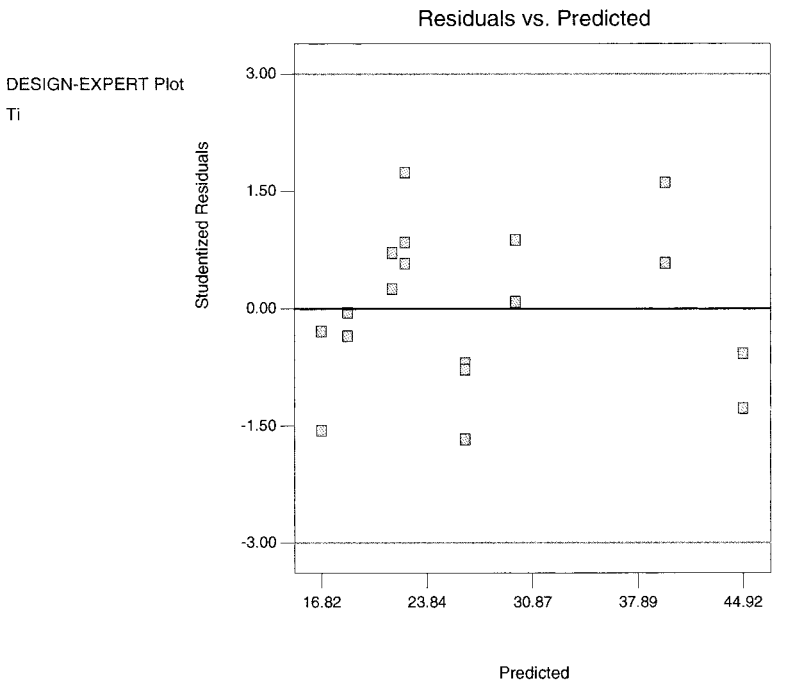

Figure 23 Residuals versus predicted for RSM P24D–P24D-d.

blackening due to the catalytic effect of $ZnCl_2$ is such a rapid process that the effect of the readdition of HCl on the polyene sequences can be considered negligible.

To conclude, the results suggest that the readdition of HCl onto the polyene sequences is responsible for the limited sequence length both in unstabilised and stabilised formulations, the effect in the latter being less important. Furthermore, the type and mechanistic action of the stabilisers involved seemed to play a significant role in the readdition. In the presence of HCl scavengers such as Ca and Zn stearates, this readdition is difficult to follow during the period of the analysis due to the fact that there is insufficient HCl formed to be readded. However, the addition of a short-term costabiliser such as P24D leads to the build-up of HCl, allowing, therefore, the readdition to take place.

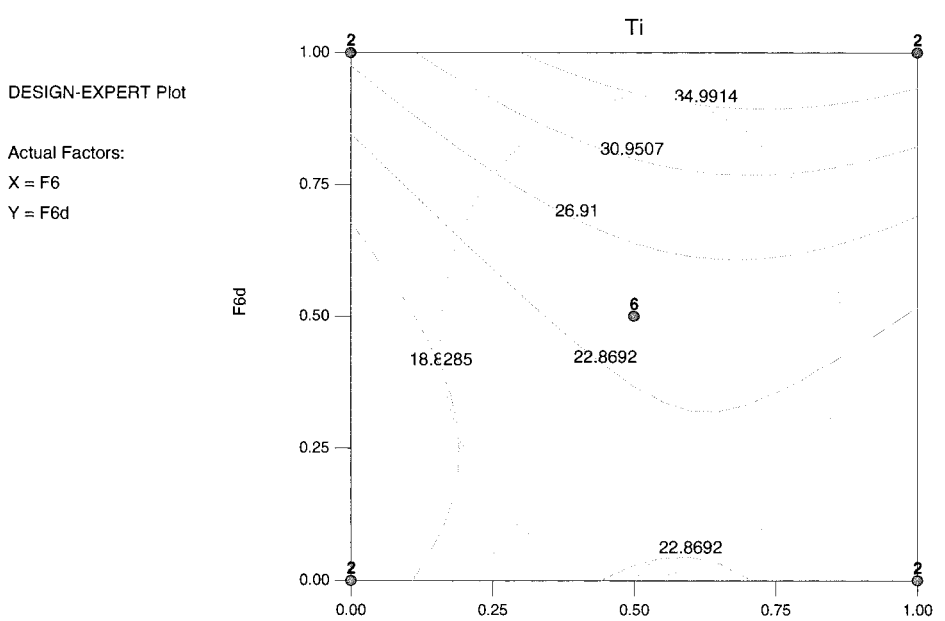

Figure 24 Model contour for RSM P24D–P24D-d.

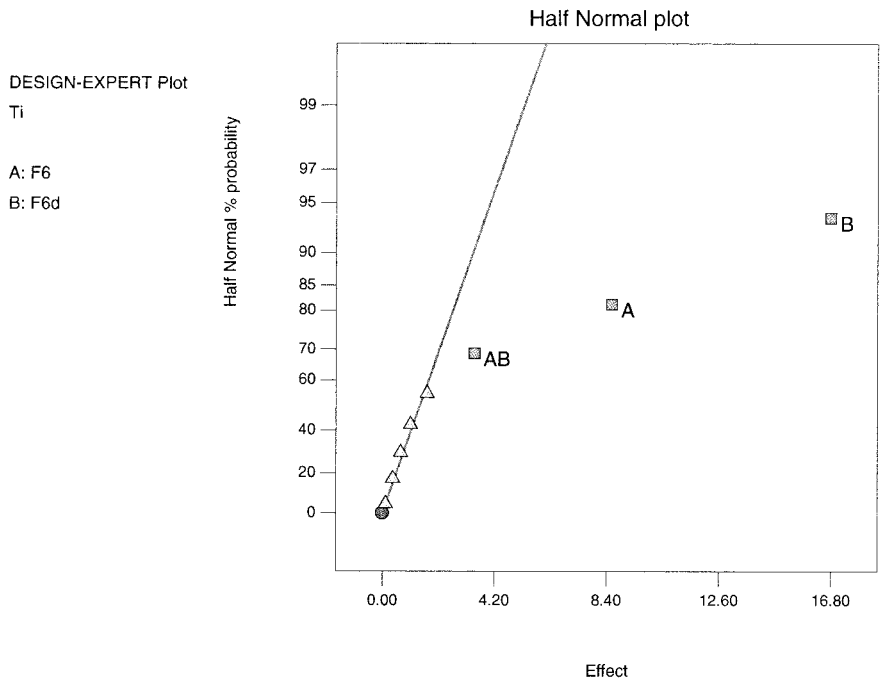

Figure 25 Half-normal probability plot for 2-LFD P24D–P24D-d.

Design of experiments

This section reports on a study of the possible synergism between P24D and P24D-d, where P24D-d upon degradation could act as a "reservoir" for P24D (Fig. 8), providing an additional extension in the induction time, as well as an improvement in the initial good color.

For this particular case, two different types of designs were performed: a response surface method (RSM) and a two-level factorial design.

Response surface method

RSM is a type of design that allows optimization of the response of interest by way of combination of several

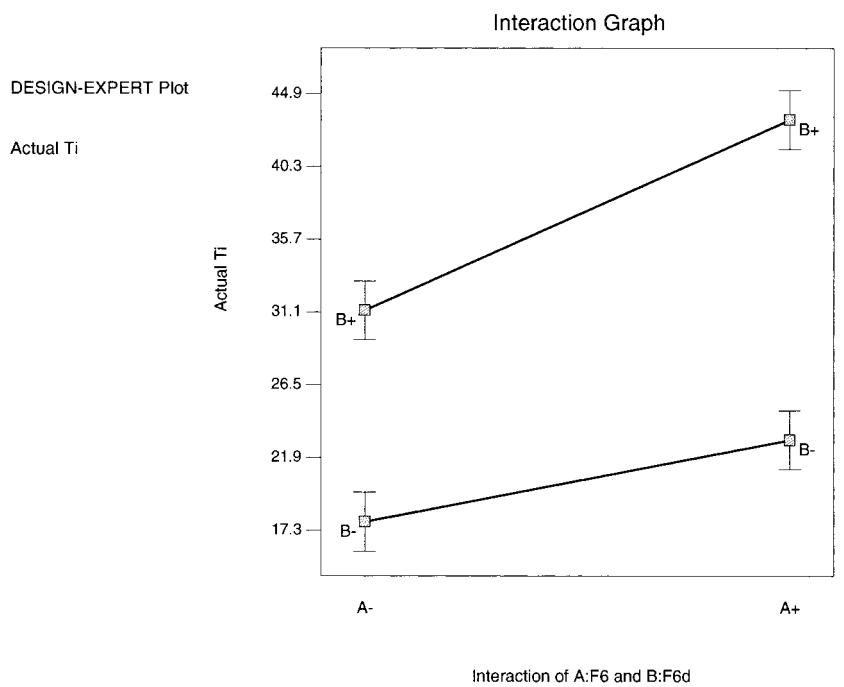

Figure 26 Interaction plot for P24D and P24D-d.

TABLE IV
Equation for Main Effects in 2-LFD P24D–P24D-d

T_i (induction time) =	+17.85 +5.15 × P24D +13.35 × P24D-d +6.90 × P24D × P24D-d

independent or controlled variables. Among the RSM designs, a standard central composite design (CCD) was chosen, being well suited for fitting quadratic surfaces.

The response opted for in this system was the T_i to DHC, with two factors, P24D and P24D-d. Contrary to the upper levels used in the previous section, an upper level of 1 phr was used to cover a wider range. The status of the design is shown in Table I.

The statistics of the different proposed models are shown in Table II. As can be seen, the quadratic model fitted the system best, exhibiting low "root MSE", high "predicted R-squared," and low "PRESS."

The ANOVA (analysis of variance) section provided an equation for the proposed quadratic model in Table III.

The first term of the equation, 16.55, refers to the presence of a mixture of Ca/Zn stearates (2 : 1) in the formulation that extends the T_i compared to the PVC alone. The negative coefficient of P24D in the square term is related to the detrimental effect that P24D may exert when present in high concentrations. The positive coefficient for P24D×P24D-d confirms the initial hypothesis of a possible synergism, with P24D-d acting as a "reservoir" of P24D on degradation. Therefore, this model confirms previous results as to the synergistic effect between P24D and P24D-d.

To validate the model, the diagnostics section displays a normal plot of the residuals (Fig. 22) with a view to elucidating whether all of the errors are equally scattered. The presence of a straight line seemed to indicate that the ANOVA assumptions were met. The "residuals versus predicted" graph (Fig. 23) showed no patterns, therefore the ANOVA assumptions were met.

In the contour graph of the model (Fig. 24) the T_i for different levels of the factors (P24D and P24D-d) is depicted: the lines represent points that take the same response values for different formulations. The circle indicates the area where the error for the response values is minimized. Because the objective of the RSM is to optimize the performance of the system, the model graph is concerned with obtaining the highest possible response value at the lowest factor concentration. Therefore, according to the plot, it would be possible to get a formulation with an induction time of 35 min with 0.90 phr of P24D-d and 0.5 phr of P24D.

Two-level factorial design

This type of design is employed to estimate separately main effects and two-factor interactions that are involved in the system. In Figure 25 the absolute values of all effects on a half-normal probability plot are shown. Only the most relevant effects fall off to the

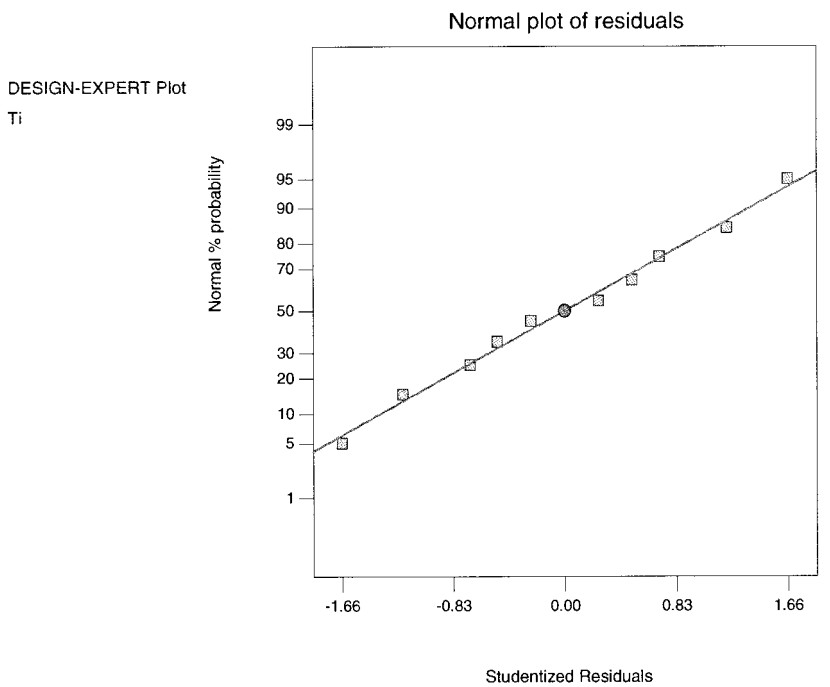

Figure 27 Normal plot of residuals for 2-LFD P24D–P24D-d.

right of the line. It appears to suggest again that there is an interaction between P24D and P24D-d and that its affect on the T_i is relatively significant.

According to the interaction plot in Figure 26, the presence of nonparallel lines confirms the interaction between P24D and P24D-d, since the effect of P24D depends on the effect of P24D-d and *vice versa.*

In Table IV the final equation in terms of factors is shown. The first term of the equation, 17.85, refers to the presence of a mixture of Ca/Zn stearates (2 : 1) in the formulation that extends the T_i compared to the PVC alone. The positive coefficient of P24D can be attributed to its interaction with the PVC chain through the C-alkylation reaction, substituting labile chlorines (see Part 1). The positive coefficient of P24D-d may be related to the fact that it decomposes rapidly and the amine gas given off neutralizes the HCl evolved. Finally, this design confirms, once again, that there is a synergistic effect taking place between P24D and P24D-d.

To validate the model, Figure 27 represents the normal plot of residuals. The lack of significant curvature in the line revealed that the ANOVA assumptions were met and therefore validated the model.

It may be concluded that P24D-d on degradation operates as a "reservoir" for P24D, extending the T_i to higher values compared to their individual performances and giving rise to a synergistic combination.

ACKNOWLEDGMENTS

The authors thank Akcros Chemicals for partial financial support of this research and Dr H. B. Harvey for useful discussions.

References

1. Geddes, W. C. Eur Polym J 1967, 3, 267.
2. Hjertberg, T.; Martinsson, E.; Sorvik, E. Macromolecules 1988, 21, 603.
3. Zafar, M. M.; Mahmood, R. Eur Polym J 1976, 12, 333.
5. Starnes, Jr., W. H.; Girois, S. Polym Yearbook, 1995, 12, 105.
5. Martinsson, E.; Hjertberg, T.; Sorvik, E. Macromolecules 1988, 21, 136.
6. Winkler, D. E. J Polym Sci 1959, 35, 3.
7. Stromberg, R. R.; Straus, S.; Achhamer, B. G. J Polym Sci 1959, 35, 355.
8. Yousufzai, A. H. K.; Zafar, M. M.; Hasan, S. U. Eur Polym J 1972, 8, 1231.
9. Stapfer, C. H.; Granick, J. D. J Polym Sci 1971, A1, 2625.
10. Kelen, T.; Balint, G.; Galambos, G.; Tudos, F. Eur Polym J 1969, 5, 597.
11. Panek, M. G.; Villacorta, G. M.; Starnes, Jr., W. H. Macromolecules 1985, 18, 1040.
12. Svetly, J.; Lukas, R.; Kolinsky, M. Makromol Chem 1979, 180, 1363.
13. Svetly, J.; Lukas, R.; Michalcova, J.; Kolinsky, M. Makromol Chem Rapid Commun 1980, 1, 247.
14. Svetly, J.; Lukas, R.; Pokorny, S., Kolinsky, M. Makromol Chem Rapid Commun 1981, 2, 149.
15. Svetly, J.; Lukas, R.; Michalcova, J.; Kolinsky, M. Makromol Chem 1979, 185, 2183.
16. Bacaloglu, R.; Fisch, M. Polym Degrad Stab 1995, 47, 33.
17. Bacaloglu, R.; Fisch, M. Polym Degrad Stab 1995, 47, 9.
18. Abbas, K. B.; Sorvik, E. M. J Appl Polym Sci 1975, 19, 2991.
19. Van Hoang, T.; Michel, A.; Guyot, A. Polym Degrad Stab 1982, 4, 365.
20. Van Hoang, T.; Guyot, A. Polym Degrad Stab 1988, 21, 165.
21. Owen, E. D.; Williams, J. I. J Polym Sci Polym Chem Ed 1974, 12, 1933.
22. Van Hoang, T.; Michel, A.; Pichot, C.; Guyot, A. Eur Polym J 1975, 11, 469.
23. Kelen, T.; Tudos, F. Macromolecular Chemistry Saarela, K., Ed.; Butterworths: London, 1973; vol. 8, p. 393.
24. Rasuvaev, G. A.; Troitskaya, L. S.; Troitskii, B. B.. J Polym Sci 1971, A1, 9, 2673.
25. Guyot A.; Bert, M. J Appl Polym Sci 1973, 17, 753.
26. Guyot A.; Michel, A. In Developments in Polymer Degradation; Scott, G., Ed.; Applied Science Publishers Ltd.: London, 1980; vol. 2, Chap. 3.
27. Nagy, T. T.; Kelen, T.; Turcsanyi, B.; Tudos, F. Polym Bull 1980, 2, 77.
28. Pern, F. J. Polym Degrad Stab 1993, 41, 125.
29. Jacques, P. P. L.; Poller, R. C. Eur Polym J 1993, 29, 1, 75.
30. Owen, E. D.; Al-Moh'd, H. S. M. Polym Degrad Stab 1997, 56, 235.
31. Owen, E. D.; Hamzeh S. M. Al-Moh'd. Polymer 1997, 38, 3533.
32. Owen, E. D.; Shah, M.; Twigg, M. V. Polym Degrad Stab 1996, 51, 151.
33. Kelen, T.; Balint, G.; Galambos, G.; Tudos, F. Eur Polym J 1969, 5, 597.
34. Van Hoang, T.; Michel, A.; Pichot, C.; Guyot, A. Eur Polym J 1975, 11, 469.
35. Kelen, T.; Balint, G.; Galambos, G.; Tudos, F. J Polym Sci 1971, C33, 211.
36. Amer, A. R.; Shapiro, J. S. J Macromol Sci Chem 1980, A14, 185.
37. James, C. E.; Poller, R. C. Eur Polym J 1986, 22, 10, 767.
38. Rabek, J. F.; Ranby, B.; Skowronski, T. A. Macromolecules 1985, 18, 1810.
39. Allen, N. S. Polym Degrad Stab 1984, 6, 193.
40. Owen, E. D.; Read, R. L. Eur Polym J 1979, 15, 41.
41. Patel, K.; Velazquez, A.; Calderon, H. S.; Brown, G. R. J Appl Polym Sci 1992, 46, 179.
42. Van Hoang, T.; Michel, A.; Guyot, A. Polym Degrad Stab 1982, 4, 365.
43. Van Hoang, T.; Guyot, A. Polym Degrad Stab 1988, 21, 165.
44. Chaudhry, H. I. PhD thesis, The Manchester Metropolitan University, 1999.
45. Benavides, R.; Edge, M.; Allen, N. S.; Shah, M. Polym Degrad Stab 1997, 57, 25.